

Molecular mechanism for hydrogen-hydrogen excitation collisions

F. Borondo, F. Martín, and M. Yáñez

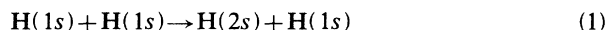
Departamento de Química, Facultad de Ciencias, C-XIV, Universidad Autónoma de Madrid, Cantoblanco, 28049 Madrid, Spain

(Received 16 April 1987)

A molecular study of the excitation reactions $H(1s)+H(1s)\rightarrow H(1s)+H(2s)$ and $H(1s)+H(1s)\rightarrow H(1s)+H(2p)$ is presented for the first time in the range of impact energies 1–9 keV, using a common translation factor to account for the momentum-transfer problem. As a consequence of this study, we explain in detail the collisional mechanisms involved and point out several new features that may explain the discrepancies between the available experimental data and all previous theoretical calculations, and among the latter. Preliminary results for the cross sections are also presented to show the influence of the form chosen for the common translation factor.

I. INTRODUCTION

Since the hydrogen-hydrogen excitation collisions



are two of the most simple conceivable nonadiabatic processes, they have received a great deal of attention from the theoretical point of view in the last fifteen years.^{1–6} In spite of this apparent simplicity there is a strong discrepancy between the available theoretical calculations for the cross sections of these two processes.

In 1954 Bates and Griffing¹ performed for the first time a calculation of the 1s-2s and 1s-2p excitation cross sections [reactions (1) and (2)] using a first-order Born approximation. Considerably later, Flannery^{2,3} and Bottcher and Flannery⁴ reported in a series of papers the most extensive and systematic study of processes (1) and (2), using the impact-parameter approximation with an atomic expansion of the electronic wave function at different levels of accuracy. The most complete one⁴ included all possible exit channels ($1s, 2s, 2p_0, 2p_{\pm 1}$), electron exchange, and nuclear symmetry, although it did not take into account the momentum transfer of the electrons. According to the authors' arguments, this latter effect should be small, since their results tended toward those of the Born approximation for reaction (1). For the particular case of reaction (1), the momentum-transfer problem was explicitly considered in a two-state impact-parameter calculation including electron exchange by Ritchie⁵ and by McLaughlin and Bell.⁶ While the former author chose the relative velocity vector along the internuclear axis (since this greatly simplifies the exchange matrix elements), the latter ones removed this approximation. Surprisingly, all reported calculated cross sections differ from each other, by up to two orders of magnitude in some cases. Furthermore, the origin of these discrepancies cannot be easily understood, since at present there is a complete lack of information on the mechanism responsible for processes (1) and (2).

Unfortunately, the experimental results do not help to

settle the controversy. The cross section for reaction (1) has been measured independently by Hill *et al.*⁷ and Morgan *et al.*,^{8,9} their results differ typically by a factor of 2 and none of the theoretical calculations are clearly privileged by any of these two sets of experimental data. Reaction (2) has only been studied experimentally by Morgan *et al.*⁸ and again there is a noticeable disagreement with the theoretical results.

The aim of this paper is to present, for the first time, a molecular treatment of the excitation processes (1) and (2), which will permit us to propose and explain the mechanisms involved in these two reactions. The lack of such a molecular treatment in the literature is due to several reasons. In first place, it implies the calculation of three quantitative correlation diagrams, namely, energies and couplings for the $^1\Sigma_g^+$, $^3\Sigma_u^+$, and $^3\Pi_u$ electronic states of the H_2 quasimolecule. In this respect, it should be noticed that, although the $^1\Sigma_g^+$ subsystem has been extensively studied and very accurate energies for the $1^3\Sigma_u^+$ and $1^3\Pi_u$ states have been reported in the literature,^{10,11} the energies for the excited $^3\Sigma_u^+$ states and their couplings have only been published very recently,¹² and those for the $^3\Pi_u$ one are not available in the literature. Secondly, the primary mechanisms of processes (1) and (2) involve, as we shall discuss later, transitions that take place at very short internuclear distances, where model potential techniques cannot be used to obtain the correlation diagram, and the only sensible alternative is performing *ab initio* calculations. Finally, the existence of constant radial couplings at infinite internuclear separation between the entrance and some exit channels requires the use of a translation factor. The choice of the functional form of this factor will be shown in Sec. IV to be a crucial problem in the study of this kind of process.

The organization of the paper is as follows. In Sec. II we briefly discuss the molecular method when a common translation factor (CTF) is included. In Sec. III we present the energies and couplings of the $^1\Sigma_g^+$, $^3\Sigma_u^+$, and $^3\Pi_u$ states of the H_2 molecule that are needed in our study. Finally, in Sec. IV we analyze the transition probabilities of processes (1) and (2) and extract the mechanisms responsible for both; we also present prelim-

inary values for the corresponding cross sections.

Atomic units will be used unless otherwise stated.

II. METHOD

In the collision energy range considered in this paper the cross sections of reactions (1) and (2) can be obtained by solving the impact-parameter equation

$$i\frac{\partial}{\partial t}\psi(\mathbf{r},t)=H_{el}\psi(\mathbf{r},t), \quad (3)$$

where H_{el} is the electronic Born-Oppenheimer Hamiltonian of the colliding system and $\psi(\mathbf{r},t)$ is the corresponding electronic wave function. As we have indicated in the Introduction, we use a molecular expansion of $\psi(\mathbf{r},t)$:

$$\psi(\mathbf{r}_1, \mathbf{r}_2, t) = e^{i[U(\mathbf{r}_1, t) + U(\mathbf{r}_2, t)]} \times \sum_j a_j(t) \chi_j(\mathbf{r}_1, \mathbf{r}_2; R) \exp\left[-i \int_0^t E_j dt'\right], \quad (4)$$

where χ_j are the eigenfunctions of H_{el} , E_j their electronic energies, and $\exp\{i[U(\mathbf{r}_1, t) + U(\mathbf{r}_2, t)]\}$ is a common translation factor (CTF)¹³ which accounts for the momentum-transfer problem. The reason for choosing a translation factor common to all χ_j is twofold.¹⁴

(i) This form has been proved to preserve the formal convergence of the molecular expansion in the limit of a complete set of electronic wave functions, χ_j , which is not the case for all other proposed methods.

(ii) The computational effort is comparable to that required for the usual perturbed-stationary-state (PSS) method, even for many-electron systems.

We have chosen for $U(\mathbf{r}, t)$ the form proposed by Errea *et al.*:¹⁴

$$U(\mathbf{r}_j, t) = f(\mathbf{r}_j, R) \mathbf{v} \cdot \mathbf{r}_j - \frac{1}{2} f^2(\mathbf{r}_j, R) v^2 t \quad (5)$$

with

$$f(\mathbf{r}_j, R) = \frac{R^2}{R^3 + \beta^3} \mathbf{r}_j \cdot \mathbf{R}, \quad (6)$$

where the origin of the electronic coordinates is placed in the middle of the internuclear axis. This particular CTF has been thoroughly tested in many one- and two-electron molecular systems.¹⁵ We shall remark that U , as chosen in Eqs. (5) and (6), depends parametrically on β , which defines the extent of a cutoff factor in the switching function $f(\mathbf{r}_j, R)$.¹⁴

When the expansion (4) is substituted in (3), assuming straight-line trajectories ($\mathbf{R} = b\hat{\mathbf{x}} + vt\hat{\mathbf{z}}$, with b the impact parameter), one gets the following system of coupled linear differential equations:

$$i\frac{da_l}{dt} = \sum_k M_{lk} a_k \exp\left[-i \int_0^t (E_k - E_l) dt'\right], \quad (7)$$

where the coupling matrix elements are given (in the molecule-fixed reference frame) by

$$M_{lk} = \left\langle \chi_l \left| -iv_z \frac{\partial}{\partial R} \right| \chi_k \right\rangle + \left\langle \chi_l \left| -\frac{iv_x}{R} iL_y \right| \chi_k \right\rangle + \left\langle \chi_l \left| \sum_{j=1}^2 A(j) \right| \chi_k \right\rangle, \quad (8)$$

where

$$A(j) = v_z^2 \left[\frac{3}{2} g^2 + g^4 \frac{R^2}{2} - 2g^3 R + g'(1 - gR) \right] z_j^2 + v_x^2 \left[\frac{g}{R} + \frac{g^2}{2} \right] x_j^2 + v_x v_z \left[g^2 - Rg^3 + g' + \frac{g}{R} \right] x_j z_j - v_x i g \left[x_j \frac{\partial}{\partial z_j} + z_j \frac{\partial}{\partial x_j} \right] + iv_z [(-2g + g^2 R) z_j - g \delta_{k,l} + \frac{1}{2} g^2 R \delta_{k,l}] \quad (9)$$

and

$$g = \frac{R^2}{R^3 + \beta^3}. \quad (10)$$

The first and second terms in Eq. (8) are, respectively, the usual radial and rotational couplings of the PSS method and the third contains the corrections to the energies and couplings introduced by the CTF.

For reasons that will become apparent in the next sections, it is useful to define a modified radial coupling

$$-iv_z \left\langle \chi_l \left| \frac{\partial}{\partial R} + \sum_{j=1}^2 \left[(2g - g^2 R) z_j \frac{\partial}{\partial z_j} \right] \right| \chi_k \right\rangle \quad (11)$$

and a modified rotational coupling

$$\frac{iv_x}{R} \left\langle \chi_l \left| iL_y - \sum_{j=1}^2 Rg \left[x_j \frac{\partial}{\partial z_j} + z_j \frac{\partial}{\partial x_j} \right] \right| \chi_k \right\rangle, \quad (12)$$

which play the same role as the corresponding radial and rotational ones in the PSS method.

Since the entrance channel of both processes (1) and (2) is a statistical mixture of singlet and triplet states, the corresponding total cross sections will be given by

$$\sigma_l = \frac{1}{4} \sigma_l^{(S)} + \frac{3}{4} \sigma_l^{(T)}. \quad (13)$$

If one neglects the spin-orbit coupling, $\sigma_l^{(S)}$ and $\sigma_l^{(T)}$ can be obtained by integration, over all impact parameters,

of the corresponding transition probabilities:

$$\sigma_l^{(S,T)} = 2\pi \int_0^\infty b P_l^{(S,T)}(b) db, \quad (14)$$

where

$$P_l^{(S,T)}(b) = \lim_{t \rightarrow \infty} |a_l^{(S,T)}(t)|^2, \quad (15)$$

which is obtained by integration of the corresponding differential equation systems (7) for the singlet and triplet subsystems.

III. ENERGIES AND COUPLINGS

A. Singlet subsystem

As we pointed out in the Introduction, the $^1\Sigma_g^+$ states of the H_2 quasimolecule have been extensively studied in the literature in the context of atomic collisions.¹⁶⁻¹⁸ To make the paper self-consistent we reproduce in Figs. 1 and 2(a) the total energies and corresponding radial couplings presented in Ref. 18. We also present here a brief discussion of the main points which are relevant to understand the mechanisms involved in reactions (1) and (2). The electronic states presented in Fig. 1 correlate in the united-atom (UA) and separate-atoms (SA) limits as indicated in Table I. The entrance channel for the reactions considered in this paper is represented asymptotically by the first state, and the exit ones by the second and the third.

We see in Fig. 2(a) that the 1-3 radial coupling between the entrance and one of the exit channels tends to a constant value as R goes to infinity; this enforces the introduction of a translation factor in the molecular expansion of the electronic wave function since, otherwise, the transition probability would oscillate with the starting point of the integration of the system of coupled equations. We have calculated the modified radial couplings [Eq. (11)] using the CTF of Eqs. (5) and (6) for different values of the parameter β in the range 1.0-3.0 and the same basis set of Ref. 18. Our results for the

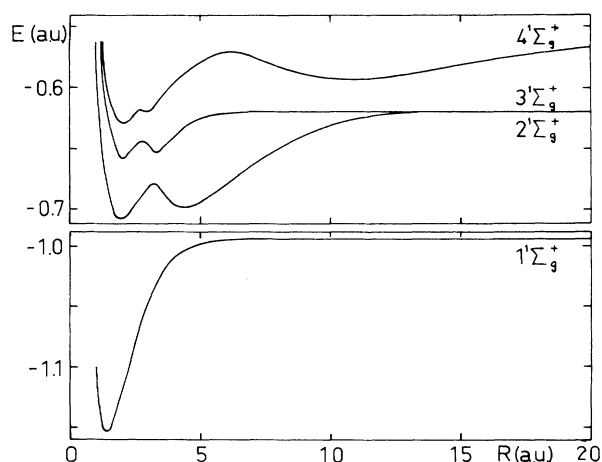


FIG. 1. Potential-energy curves for the first four $^1\Sigma_g^+$ states of the H_2 molecule.

TABLE I. United-atom (UA) and separate-atom (SA) limits of the first four $^1\Sigma_g^+$ of H_2 .

UA	State	SA
$1s^2$	$1^1\Sigma_g^+$	$H(1s) + H(1s)$
$1s2s$	$2^1\Sigma_g^+$	$H(1s) + H(2s)$
$1s3s$	$3^1\Sigma_g^+$	$H(1s) + H(2p)$
$1s3d$	$4^1\Sigma_g^+$	$H^+ + H^-(1s^2)$

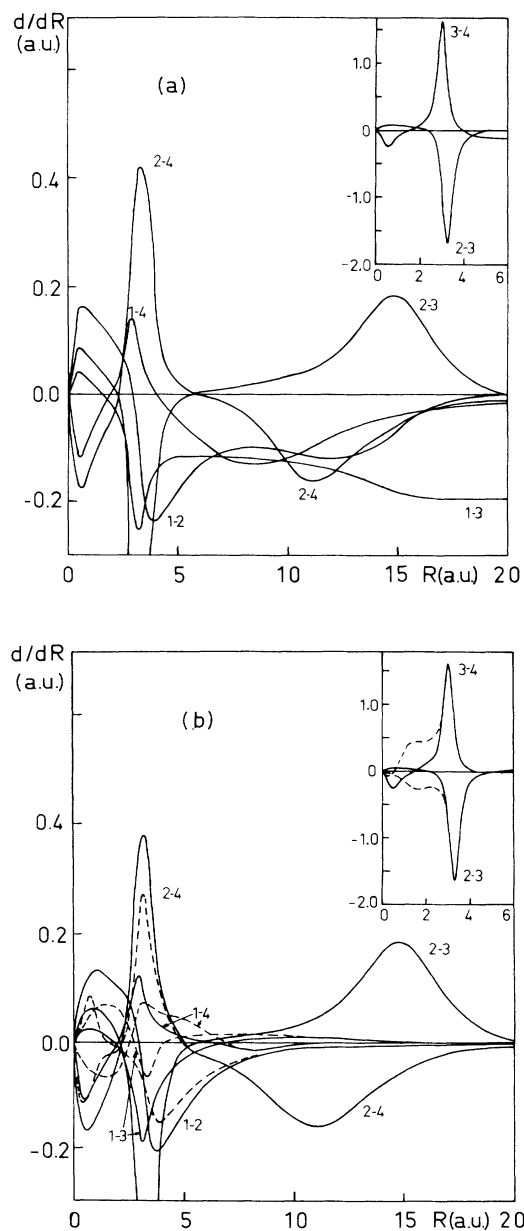


FIG. 2. (a) Radial couplings between the first four $^1\Sigma_g^+$ states of the H_2 molecule. (b) Modified radial couplings [Eq. (11)] between the first four $^1\Sigma_g^+$ states of the H_2 molecule for $\beta=3.0$ (—) and $\beta=1.0$ (---). For clarity, the 2-3 and 3-4 radial couplings have been drawn in a different scale.

two extreme values of β are presented in Fig. 2(b). The main features of this figure relevant to our study can be summarized as follows.

(i) The entrance channel only has a significant coupling with the $2^1\Sigma_g^+$ state, which presents a peak at $R \approx 4$ a.u.

(ii) The exit channel $2^1\Sigma_g^+$ presents a Nikitin-Demkov-type¹⁹ coupling with the $4^1\Sigma_g^+$ at $R \sim 11$ a.u., due to the exponential interaction between the corresponding "ionic" and "covalent" diabatic states.¹⁷

(iii) There is a coupling between the two exit channels, $2^1\Sigma_g^+$ and $3^1\Sigma_g^+$, of area $\pi/4$ due to the Stark mixture of the $2s$ and $2p$ atomic orbitals, induced by the exponentially decreasing electric field of the H($1s$) atom.^{17,20}

B. Triplet subsystem

In a previous paper,¹² we have calculated the potential energy curves of the $3^3\Sigma_u^+$ states of H_2 and their radial couplings, which are needed in the present molecular study of reactions (1) and (2), and analyzed in detail the relevant features of the correlation diagram. We show these energies and couplings in Figs. 3 and 4(a), respectively. The electronic states presented in Fig. 3 correlate in the UA and SA limits as indicated in Table II. The entrance channel is represented asymptotically by the first state, and the exit ones by the second and the third.

As in the singlet subsystem, we can see in Fig. 4(a) that the 1-3 radial coupling tends to a constant value as R goes to infinity. Consequently, we have calculated the modified radial couplings [Eq. (11)] using the same CTF as in the previous case for values of β in the range 1.0–3.0 and the same basis set of Ref. 12. Our results for the extreme values of β are shown in Fig. 4(b). The most significant features of this figure are as follows.

(i) All radial couplings involving the entrance channel, $1^3\Sigma_u^+$, are practically cancelled by the CTF for inter-

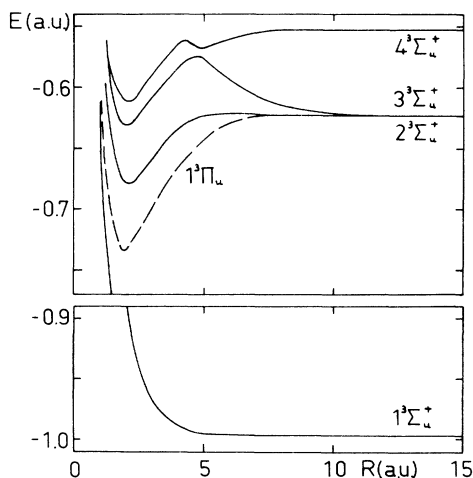


FIG. 3. Potential-energy curves for the first four $3^3\Sigma_u^+$ (—) and the first $3^1\Pi_u$ (---) state of the H_2 molecule.

TABLE II. United-atom (UA) and separate-atom (SA) limits of the first four $3^3\Sigma_u^+$ of H_2 .

UA	State	SA
$1s2p$	$1^3\Sigma_u^+$	H($1s$) + H($1s$)
$1s3p$	$2^3\Sigma_u^+$	H($1s$) + H($2s$)
$1s4p$	$3^3\Sigma_u^+$	H($1s$) + H($2p$)
$1s4f$	$4^3\Sigma_u^+$	H($1s$) + H($3s$)

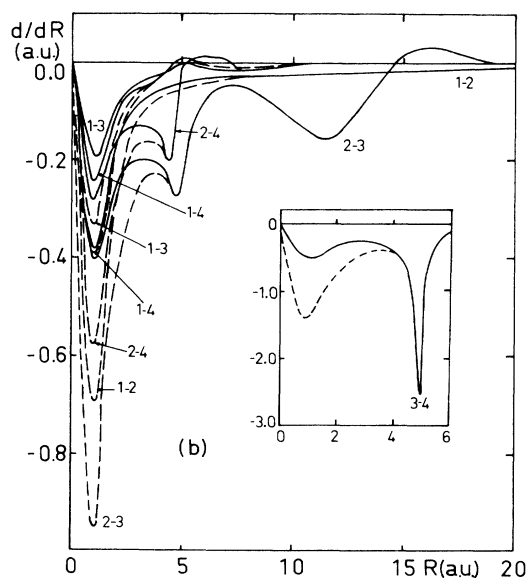
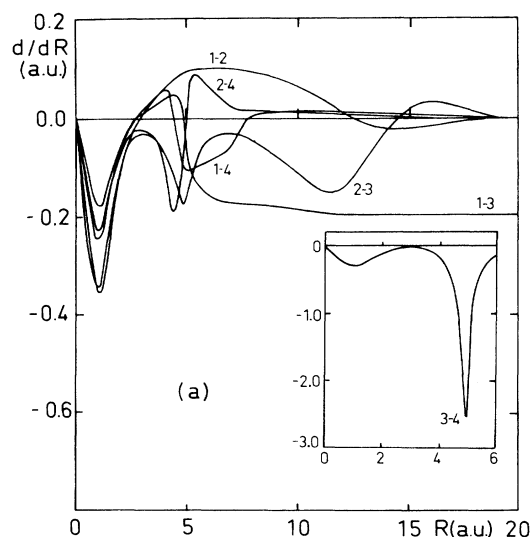


FIG. 4. (a) Radial couplings between the first four $3^3\Sigma_u^+$ states of the H_2 molecule. (b) Modified radial couplings [Eq. (11)] between the first four $3^3\Sigma_u^+$ states of the H_2 molecule for $\beta=3.0$ (—) and $\beta=1.0$ (---). For clarity, the 3-4 radial coupling has been drawn in a different scale.

TABLE III. United-atom (UA) and separate-atom (SA) limits of $1^3\Sigma_u^+$ and $1^3\Pi_u$ of H_2 .

UA	State	SA
$1s2p$	$1^3\Sigma_u^+$	$H(1s) + H(1s)$
$1s2p$	$1^3\Pi_u$	$H(1s) + H(2p)$

mediate and long internuclear distances, being only important for $R \simeq 1$ a.u. This holds for all values of β in the range considered here.

(ii) There exists a strong coupling at $R \sim 12$ a.u. between the two exit channels, $2^3\Sigma_u^+$ and $3^3\Sigma_u^+$, which is the result of the competition between the $2s$ - $2p$ Stark mixing effect (also present in the singlet case) and the promotion effect of the inner orbital.¹²

In addition to the radial couplings mentioned in (i), the entrance channel can also be coupled rotationally with states of $^3\Pi_u$ symmetry. In fact, in this case, the $1^3\Pi_u$ becomes degenerate with the entrance channel in the UA limit (see Table III), indicating that one can expect an effective coupling between them.

To calculate the energies and couplings of the $^3\Pi_u$ subsystem we have used a configuration-interaction (CI) method with the basis set of Gaussian-type orbitals (GTO's) presented in Table IV. The main conclusions of this calculation is that the radial couplings involving the $1^3\Pi_u$ state are smaller than 10^{-3} a.u. in the whole range of internuclear distances. On the other hand, the influence of rotational couplings between higher $^3\Pi_u$ states and the lowest $^3\Sigma_u^+$ state should be completely negligible since all these couplings tend to zero in the vicinity of the UA limit, where the remaining ones are relevant. Similarly, the rotational couplings between excited $^3\Pi_u$ and $^3\Sigma_u^+$ states should be inefficient since the excited $^3\Sigma_u^+$ become populated only at the exit of the

TABLE IV. Exponents of the Gaussian orbitals used in the molecular calculations of the $^3\Pi_u$ states for (a) $R < 5.0$ a.u. and (b) $R > 5.0$ a.u.

α_{1s}	α_{2p_z}	α_{2p_x}
	(a)	
0.17	0.02	0.004
0.65	0.1	0.02
2.3	0.5	0.1
8.0		0.5
	(b)	
0.092	0.02	0.004
0.45	0.1	0.02
2.0	0.5	0.1
8.0		0.5

collision. Accordingly, one needs to include only the first $^3\Pi_u$ state in the molecular study of reactions (1) and (2). Its energy curve is shown (dashed line) in Fig. 3. With respect to the accuracy of our calculation of the $1^3\Pi_u$ state, it should be noticed that (i) our energies compare quite well with the very accurate values reported by Kolos and Rychlewski,¹¹ the difference being always smaller than 10^{-3} a.u., (ii) the energy differences between our $1^3\Sigma_u^+$ and $1^3\Pi_u$ states coincide within an error of 10^{-3} a.u., with those obtained from Refs. 10 and 11, and (iii) the energy curves of the $2^3\Sigma_u^+$, $3^3\Sigma_u^+$, and $1^3\Pi_u$ states are completely degenerate at $R = \infty$ ($\Delta E < 10^{-5}$ a.u.).

The rotational couplings between the $1^3\Pi_u$ state and the four $^3\Sigma_u^+$ states of Fig. 3 are presented in Fig. 5(a). It can be observed that all these couplings tend to zero in the UA limit, except the $\langle 1^3\Sigma_u^+ | iL_y | 1^3\Pi_u \rangle$ that goes to unity:

$$\begin{aligned} \langle 1^3\Sigma_u^+ | iL_y | 1^3\Pi_u \rangle_{R \rightarrow 0} &\sim \left\langle \frac{1}{\sqrt{2}}(1s2p_x - 2p_x 1s) \left| iL_y(1) + iL_y(2) \right| \frac{1}{\sqrt{2}}(1s2p_z - 2p_z 1s) \right\rangle \\ &= \langle 2p_x | iL_y | 2p_z \rangle = 1 \end{aligned} \quad (16)$$

in an obvious notation. A rather conspicuous feature of this coupling is that it increases linearly in the asymptotic region. This behavior is easily understood when one considers the asymptotic expression of the corresponding wave functions:

$$\begin{aligned} \langle 1^3\Sigma_u^+ | iL_y | 1^3\Pi_u \rangle_{R \rightarrow \infty} &\sim \left\langle \frac{1}{\sqrt{2}}(1s_A 1s_B - 1s_B 1s_A) \left| iL_y(1) + iL_y(2) \right| \frac{1}{2}(1s_A 2p_{xB} + 1s_B 2p_{xA} - 2p_{xB} 1s_A - 2p_{xA} 1s_B) \right\rangle \\ &= \frac{1}{\sqrt{2}}(E_{1s} - E_{2p}) \langle 2p_x | x | 1s \rangle R. \end{aligned} \quad (17)$$

By similar arguments it can also be shown that the $\langle 3^3\Sigma_u^+ | iL_y | 1^3\Pi_u \rangle$ coupling tends to one as $R \rightarrow \infty$. On the other hand, the $\langle 3^3\Sigma_u^+ | iL_y | 1^3\Pi_u \rangle$ and $\langle 4^3\Sigma_u^+ | iL_y | 1^3\Pi_u \rangle$ present a steplike behavior at $R \simeq 5$

a.u. due to the exchange of character of the wave functions of the corresponding Σ states at the avoided crossing between their energy curves.

In Fig. 5(b) we show the rotational couplings correct-

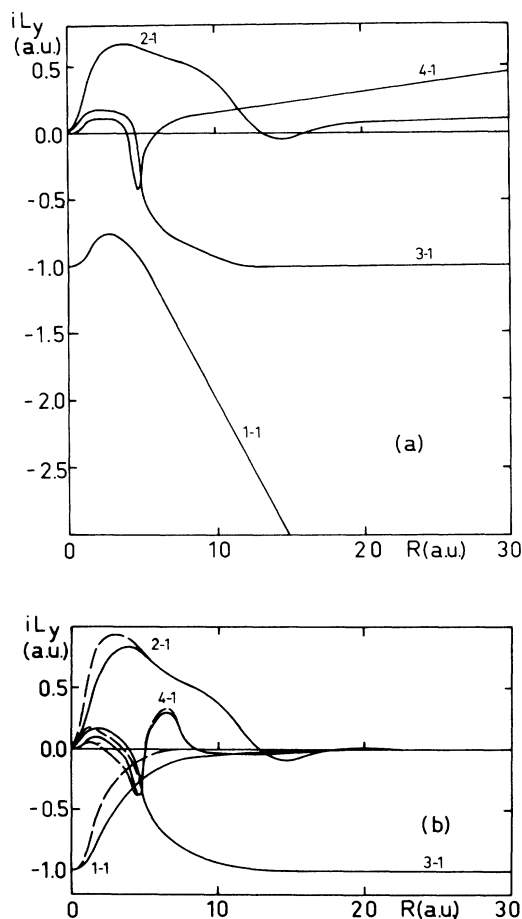


FIG. 5. (a) Rotational couplings between the first four ${}^3\Sigma_u^+$ states and the first ${}^3\Pi_u$ state of the H_2 molecule. (b) Modified rotational couplings [Eq. (12)] between the first four ${}^3\Sigma_u^+$ states and the first ${}^3\Pi_u$ state of the H_2 molecule for $\beta=3.0$ (—) and $\beta=1.0$ (---).

ed by the inclusion of the CTF [see Eq. (12)]. We see that the unphysical behavior of the $\langle 1^3\Sigma_u^+ | iL_y | 1^3\Pi_u \rangle$ (similar to the existence of constant radial couplings as infinity) has disappeared; also, the $\langle 2^3\Sigma_u^+ | iL_y | 1^3\Pi_u \rangle$ coupling is very important at intermediate internuclear distances.

IV. MOLECULAR MECHANISM

According to the analysis presented in Sec. III, we can conclude that a molecular expansion of the electronic wave function (4) (that accounts for the strong couplings between all exit channels) must include, at least, the first four ${}^1\Sigma_g^+$ states, the first four ${}^3\Sigma_u^+$ states and the first ${}^3\Pi_u$ state of the H_2 molecule. In other words, it is not possible to study separately the two excitation processes (1) and (2). However, this point is not clear in the literature, and, with the exceptions of the works of Flannery³ and Bottcher and Flannery,⁴ most of the calculations using atomic expansions do not include simultaneously all

possible exit channels of reactions (1) and (2). To elucidate the mechanism responsible for these two processes, we have carried out calculations of the transition probabilities at different impact energies, and for different values of the parameter β . For this purpose, we have used the program PAMPA²¹ to integrate the system of differential equations (7), conveniently modified to include the new elements introduced by the CTF.

In Fig. 6 we plot the transition probabilities²²

$$P_{2s}^S(b) = \frac{1}{2} |a_{2^1\Sigma_g^+}(t = \infty)|^2,$$

$$P_{2p}^S(b) = \frac{1}{2} |a_{3^1\Sigma_g^+}(t = \infty)|^2,$$

$$P_{2s}^T(b) = \frac{1}{2} |a_{2^3\Sigma_u^+}(t = \infty)|^2,$$

$$P_{2p}^T(b) = \frac{1}{2} |a_{3^3\Sigma_u^+}(t = \infty)|^2 + \frac{1}{2} |a_{1^3\Pi_u}(t = \infty)|^2 \quad (18)$$

times the impact parameter b , as functions of b for an impact energy of 2.25 keV and for two different values of β . A similar plot is presented in Fig. 7 for an impact energy of 9 keV. Although these figures show that the transition probabilities are very strongly β dependent in magnitude, there exist several patterns that do not change significantly with β , namely, (i) in the triplet subsystem, both for the $1s$ - $2s$ and the $1s$ - $2p$ excitations, all transitions take place at impact parameters smaller than 2 a.u. This is in good agreement with all previous atomic theoretical calculations; (ii) on the contrary, in singlet

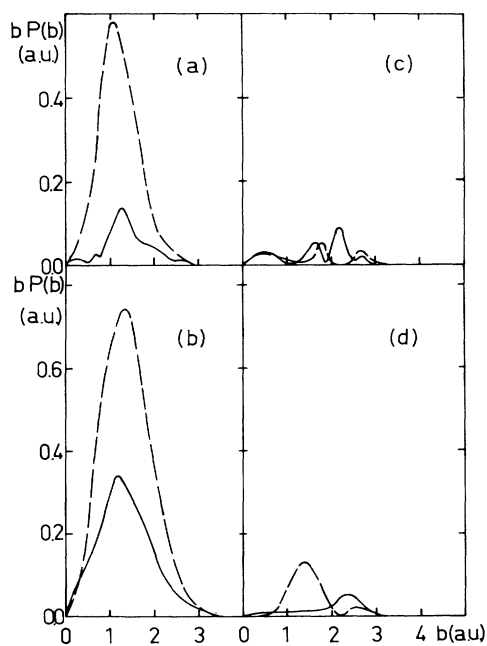


FIG. 6. Plot of transition probabilities times the impact parameter b vs b for $E = 2.25$ keV. (a) (—) $bP_{2s}^T(b)$, (---) $bP_{2p}^T(b)$ for $\beta=1.0$; (b) (—) $bP_{2s}^T(b)$, (---) $bP_{2p}^T(b)$ for $\beta=3.0$; (c) (—) $bP_{2s}^S(b)$, (---) $bP_{2p}^S(b)$ for $\beta=1.0$; (d) (—) $bP_{2s}^S(b)$, (---) $bP_{2p}^S(b)$ for $\beta=3.0$.

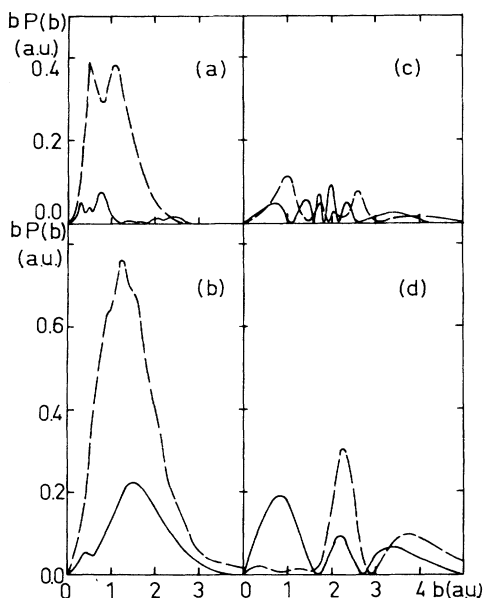


FIG. 7. Plot of transition probabilities times the impact parameter b vs b for $E=9.0$ keV. (a) (—) $bP_{2s}^T(b)$, (---) $bP_{2p}^T(b)$ for $\beta=1.0$; (b) (—) $bP_{2s}^T(b)$, (---) $bP_{2p}^T(b)$ for $\beta=3.0$; (c) (—) $bP_{2s}^S(b)$, (---) $bP_{2p}^S(b)$ for $\beta=1.0$; (d) (—) $bP_{2s}^S(b)$, (---) $bP_{2p}^S(b)$ for $\beta=3.0$.

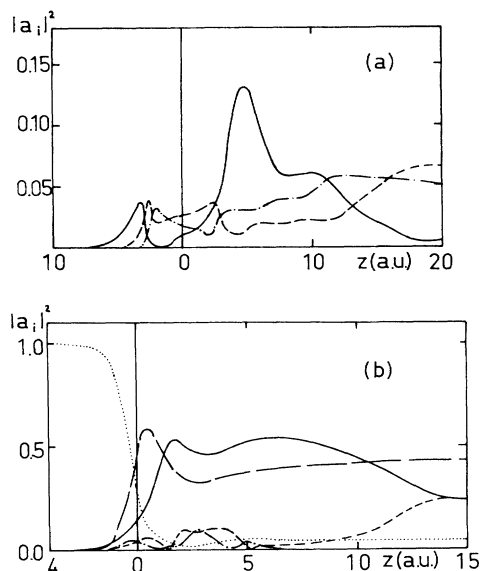


FIG. 8. Plot of the values of the transition probabilities $|a_j(t)|^2$ vs $z=vt$. (a) Singlet subsystem, $j=2^1\Sigma_g^+$ (—), $3^1\Sigma_g^+$ (---), $4^1\Sigma_g^+$ (-.-.-), for $E=6.25$ keV, $b=1.6$ a.u., and $\beta=3.0$. (b) Triplet subsystem, $j=1^3\Sigma_u^+$ (⋯), $2^3\Sigma_u^+$ (—), $3^3\Sigma_u^+$ (---), $4^3\Sigma_u^+$ (-.-.-), $1^3\Pi_u$ (---), for $E=6.25$ keV, $b=1.0$ a.u., and $\beta=3.0$.

subsystem, there is a significant contribution of higher impact parameters (up to 5 a.u. for $E=9$ keV) to the excitation processes (1) and (2). These results contrast with those obtained by Ritchie⁵ and McLaughlin and Bell,⁶ who found that only impact parameters smaller than 2 a.u. were important; (iii) the main contribution to the $1s-2p$ excitation comes from the triplet subsystem; (iv) at low impact velocities the excitation $1s-2s$ occurs mainly in the triplet subsystem, while at high energies the singlet and triplet contributions are comparable. This result is in qualitative agreement with those of Ritchie,⁵ and disagrees with those of McLaughlin and Bell,⁶ and (v) although we have not separated the Σ and Π contributions to the $1s-2p$ excitation of Figs. 6 and 7 [see Eq. (18)], it must be noticed that in the triplet subsystem the Π contribution always predominates over the Σ counterpart, in agreement with the conclusion of Bottcher and Flannery.⁴

The “history” of the collision processes is displayed in Fig. 8(a) (singlet) and 8(b) (triplet), where we plot the values of the transition probabilities $|a_j(t)|^2$ as functions of the collision path $z=vt=[R^2(t)-b^2]^{1/2}$ for trajectories with $E=2.25$ keV, $\beta=3$, and values of b (1.6 a.u. for singlet and 1.0 for triplet) where the corresponding transition probabilities present maxima (see Fig. 6).

A. Singlet subsystem

For the singlet subsystem, Fig. 8(a) shows that, when the two H atoms approach, the $2^1\Sigma_g^+$ begins to be populated at $z \approx -5$ a.u. due to the $\langle 1^1\Sigma_g^+ | d/dR | 2^1\Sigma_g^+ \rangle$ coupling [see Fig. 2(b)]; then its population passes to higher states due to the series of avoided crossings at $R < 3.5$ a.u. (see Fig. 1). At the exit of the collision the $\langle 1^1\Sigma_g^+ | d/dR | 2^1\Sigma_g^+ \rangle$ coupling repopulates the $2^1\Sigma_g^+$ state at $z \approx 5$ a.u. Later, at $z \approx 11$ a.u., part of its population goes to the $4^1\Sigma_g^+$ because of the $\langle 2^1\Sigma_g^+ | d/dR | 4^2\Sigma_g^+ \rangle$ coupling. Finally, the $\langle 2^1\Sigma_g^+ | d/dR | 3^1\Sigma_g^+ \rangle$ coupling is responsible for the sharing of population between the $2^1\Sigma_g^+$ and the $3^1\Sigma_g^+$ states. This mechanism does not change significantly for other values of β .

At this point three remarks are relevant. First, the strong $\langle 2^1\Sigma_g^+ | d/dR | 3^1\Sigma_g^+ \rangle$ interaction, which controls the final relative transition probabilities for the excitations (1) and (2), does not allow, as we mentioned above, these two processes to be studied separately. Second, the $4^1\Sigma_g^+$ state [which diabatically correlates to $H^+ + H^-(1s^2)$] plays a fundamental role in the study of these two processes, since it sensibly decreases the final occupation of the $2^1\Sigma_g^+$ state; in fact, this is the predominant effect at higher velocities (see Fig. 6 of Ref. 18). And third, atomic calculations not including ionic channels cannot give a good description of the $1^1\Sigma_g^+ - 2^1\Sigma_g^+$ interaction (primary mechanism), since for $R < 10$ a.u. the character of the $2^1\Sigma_g^+$ state is roughly 50% ionic.¹⁷ Moreover, the position of the peak of the corresponding

radial coupling explains why our $bP_j(b)$ curves extend to impact parameters greater than those reported by other authors.

B. Triplet subsystem

The mechanism for the triplet subsystem is quite different. Figure 8(b) shows that the $1^3\Pi_u$ state becomes significantly populated at $z \approx 0$, through the rotational interaction with the entrance channel [see Fig. 5(b)]; afterwards, its coupling with the $2^3\Sigma_u^+$ state reduces its final occupation. Then, the population so reached by the $2^3\Sigma_u^+$ state is shared with the $3^3\Sigma_u^+$ at $z \approx 10$ a.u. due to the $\langle 2^3\Sigma_u^+ | d/dR | 3^3\Sigma_u^+ \rangle$ coupling. The previous sketched mechanism does not change significantly with the value of β . The above discussion indicates that the excitation mechanism for the triplet subsystem is mainly determined by two facts: the crucial role played by the $1^3\Pi_u$ state, which accounts for the primary mechanism, and the strong $\langle 2^3\Sigma_u^+ | d/dR | 3^3\Sigma_u^+ \rangle$ coupling, which is responsible for the final relative population of the two exit channels. The latter implies that, as in the singlet subsystem, the two excitation reactions must be studied simultaneously.

We conclude this section by presenting in Fig. 9(a)

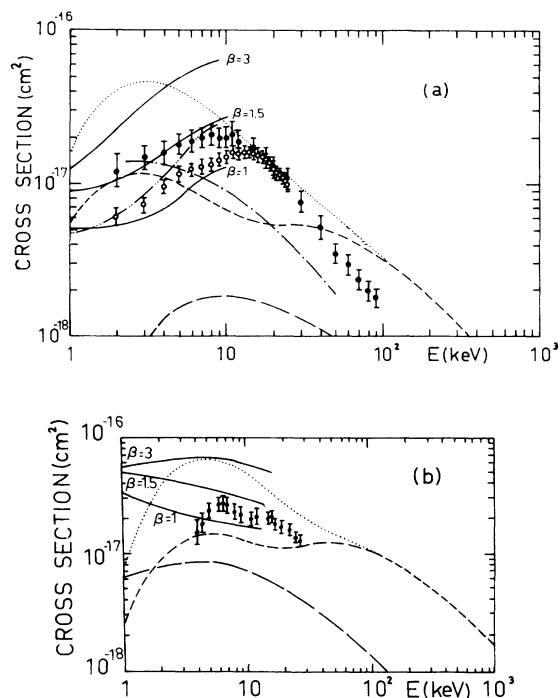


FIG. 9. Cross sections for the reactions (a) $\text{H}(1s) + \text{H}(1s) \rightarrow \text{H}(1s) + \text{H}(2s)$; (—), our results for $\beta = 1.0, 1.5,$ and 3.0 ; (---), Bates and Griffing;¹ (- - -), Bottcher and Flannery;⁴ (- · - · -), Ritchie;⁵ (· · · · ·), McLaughlin and Bell;²³ (- · - · -), McLaughlin and Bell;⁶ \square , Hill *et al.*;⁷ \circ , Morgan *et al.*;⁹ and (b) $\text{H}(1s) + \text{H}(1s) \rightarrow \text{H}(1s) + \text{H}(2p)$; (—), our results for $\beta = 1.0, 1.5,$ and 3.0 ; (---), Bates and Griffing;¹ (- - -), Bottcher and Flannery;⁴ (· · · · ·), McLaughlin and Bell;²³ \square , Morgan *et al.*⁸

and 9(b) preliminary calculated cross sections for the excitation processes (1) and (2) obtained with different values of the parameter β with the CTF of Eqs. (5) and (6). Our results are compared with the experimental values of Hill *et al.*⁷ and Morgan *et al.*⁹ for the $1s$ - $2s$ excitation, and of Morgan *et al.*⁸ for the $1s$ - $2p$ excitation; we have also included in this figure other theoretical calculations. This figure shows that our cross sections depend considerably on β , although the mechanism does not. At this point some remarks regarding this dependence may be appropriate. Usually, the modified dynamical couplings depend on β in the vicinity of the UA limit. This is a consequence of the different extension of the region (given by the values of β) in which the standard PSS expansion is preserved [see Eqs. (4)–(6)]. When the primary transitions take place outside this region, this dependence does not necessarily result in a similar one of the total cross section. This is, for instance, the case in the ion pair formation reaction in $\text{H} + \text{H}$ collisions.¹⁸ However, as indicated above, the primary transitions for the excitation reactions (1) and (2) occur in the region of very small internuclear distances, where the β dependence is notorious. More specifically, this dependence comes almost entirely from the triplet subsystem, where the parameter β controls basically the order of magnitude of the corresponding cross section. In particular, it arises from the $\langle 1^3\Sigma_u^+ | iL_y | 1^3\Pi_u \rangle$ rotational coupling that, although it is not strongly β dependent, it is very effective since the $1^3\Sigma_u^+$ and $1^3\Pi_u$ are nearly degenerate in the vicinity of the UA. Clearly, in this case, an optimization procedure of β , i.e., an optimization of the form of the CTF, is needed. However, as this is not the case for most collisional processes, very few attempts of this kind have been carried out. Among all proposed methods,²⁴ the one based on the use of a ponderated Euclidean norm of Riera²⁵ has the advantage that it can be easily implemented (as compared, for example, to variational optimization²⁴ of transition probabilities) in our case. Nevertheless, this is not a trivial extension of the present work,²⁶ and it will be considered in a future publication. On the other hand, for a wide range of values of β , our results behave as the experimental ones, especially for the $1s$ - $2s$ excitation; this can be taken as an additional indication of the feasibility of the mechanisms proposed in this paper.

V. CONCLUDING REMARKS

In this paper we have proposed molecular mechanisms for the $1s$ - $2s$ and $1s$ - $2p$ excitation processes in hydrogen-hydrogen collisions [reactions (1) and (2)]. The most relevant features can be summarized as follows. First, the two excitation reactions cannot be studied separately because of the strong interaction of the two exit channels, both for singlet and triplet subsystems at large internuclear distances. Second, the primary transitions occur at short internuclear distances due to a radial coupling at $R \approx 4$ a.u. in the singlet case and to a rotational one at $R \approx 1$ a.u. for the triplet subsystem. As a consequence of the partial ionic character of the $2^1\Sigma_g^+$ state at

$R < 10$ a.u., we have found that these primary transitions in the singlet case take place at larger impact parameters than those reported previously, and that this exit channel interacts with the $4^1\Sigma_g^+$ state, which has an asymptotic ionic character. Finally, our conclusions show that the main contribution to the $1s-2p$ excitation comes from the triplet subsystem, and that this is so for the $1s-2s$ excitation at low impact energies, while at high energies the singlet and triplet contributions are similar.

Our preliminary results for the cross sections show an important dependence on the form of the CTF chosen in the expansion of the wave function, indicating that an optimization of this form—such as that proposed by Riera²⁵—is unavoidable. Of course, an alternative procedure would be to increase the molecular expansion (4) until Galilean invariance of the cross sections were achieved. However, this type of calculation would be

much more expensive and would not provide further insight on the physics of the problem.

It is clear that new experimental measurements, specially for the $1s-2p$ excitation process, are needed in order to clarify the controversy in the different theoretical results, including ours. To be more concrete, our results for the $1s-2p$ excitation at low impact energies disagree with the experimental ones for all values of the parameters β , showing that this disagreement cannot be due to the specific form chosen for the CTF.

ACKNOWLEDGMENTS

This work was supported in part by the Comisión Asesora de Investigación Científica y Tecnológica (Spain), Project No. 890/84. We thank Professor A. Riera for helpful discussions.

-
- ¹D. R. Bates and G. W. Griffing, Proc. Phys. Soc. London, Sect. A **67**, 663 (1954).
²M. R. Flannery, Phys. Rev. **183**, 231 (1969); **183**, 241 (1969).
³M. R. Flannery, J. Phys. B **3**, L97 (1970).
⁴C. Bottcher and M. R. Flannery, J. Phys. B **3**, 1600 (1970).
⁵B. Ritchie, Phys. Rev. A **3**, 656 (1971).
⁶B. M. McLaughlin and K. L. Bell, J. Phys. B **18**, L771 (1985).
⁷J. Hill, J. Geddes, and H. B. Gilbody, J. Phys. B **12**, 2875 (1979).
⁸T. J. Morgan, J. Geddes, and H. B. Gilbody, J. Phys. B **7**, 142 (1974).
⁹T. J. Morgan, J. Stone, and R. Mayo, Phys. Rev. A **22**, 1460 (1980).
¹⁰W. Kolos and L. Wolniewicz, J. Chem. Phys. **43**, 2429 (1965); Chem. Phys. Lett. **24**, 457 (1974).
¹¹W. Kolos and J. Rychlewski, J. Mol. Spectrosc. **66**, 428 (1977).
¹²F. Borondo, F. Martín, and M. Yáñez, J. Chem. Phys. **86**, 4982 (1987).
¹³S. B. Schneiderman and A. Russek, Phys. Rev. **181**, 311 (1969).
¹⁴L. F. Errea, L. Méndez, and A. Riera, J. Phys. B **15**, 101 (1980).
¹⁵F. Martín, A. Riera, and M. Yáñez, Phys. Rev. A **34**, 4675 (1986); L. F. Errea, F. Martín, L. Méndez, A. Riera, and M. Yáñez, J. Chem. Phys. **84**, 5422 (1986); J. Hanssen, R. Gayet, C. Harel, and A. Salin, J. Phys. B **24**, L323 (1984); L. F. Errea, L. Méndez, A. Riera, M. Yáñez, J. Hanssen, C. Harel, and A. Salin, J. Phys. (Paris) **46**, 709 (1985); **46**, 719 (1985); R. J. Allan, A. Bahring, and J. Hanssen, J. Phys. B **18**, 1994 (1985); R. J. Allan and H. J. Korsch, Z. Phys. A **320**, 191 (1985); M. C. Van Hemert and E. F. Van Dishoek, Phys. Rev. A **31**, 2227 (1985).
¹⁶F. Borondo, A. Macías, and A. Riera, Phys. Rev. Lett. **46**, 420 (1981); Chem. Phys. Lett. **100**, 63 (1983).
¹⁷F. Borondo, A. Macías, and A. Riera, J. Chem. Phys. **74**, 6126 (1981); Chem. Phys. **81**, 303 (1983).
¹⁸F. Borondo, F. Martín, and M. Yáñez, Phys. Rev. A **35**, 60 (1987).
¹⁹E. E. Nikitin, Adv. Quantum Chem. **5**, 185 (1970).
²⁰F. Borondo, L. R. Eguiaray, and A. Riera, J. Phys. B **15**, 899 (1982).
²¹C. Gaussorgues, R. D. Piacentini, and A. Salin, Comput. Phys. Commun. **10**, 223 (1981).
²²A factor $\frac{1}{2}$ has to be included in Eq. (15) because the physical exit channels are (normalized) linear combinations (additions or subtractions) of the corresponding gerade and ungerade states.
²³B. M. McLaughlin and K. L. Bell, J. Phys. B **16**, 3797 (1983).
²⁴M. E. Riley and T. A. Green, Phys. Rev. A **4**, 619 (1971); V. H. Ponce, J. Phys. B **12**, 3731 (1979); **14**, 2823 (1981); D. S. F. Crothers and N. R. Todd, *ibid.* **14**, 2233 (1981); J. Rankin and W. R. Thorson, Phys. Rev. A **18**, 1990 (1978).
²⁵A. Riera, Phys. Rev. A **30**, 2304 (1984).
²⁶L. F. Errea, J. M. Gómez-Llorente, L. Méndez, and A. Riera, Phys. Rev. A **32**, 2158 (1985); **35**, 4060 (1987).